Optimization of CO_2 Absorption Using Advanced Control and Selective Amine and Demineralized Water Make-up System

Uche Noel P. Ajie[1] Emeka J. Okafor[1] and Dulu Appah[1]
[1] Petroleum and Gas Engineering Department,
University of Port-Harcourt, Choba, Nigeria.
*Corresponding Author Email Address: uche.ajie@eni.com
DOI:10.56201/ijemt.v10.no9.2024.pg53.72

Abstract
The paper presents the optimization of CO_2 mass transfer using a selective makeup advanced process control, leading to improved efficiency and reduced energy consumption in an Absorption Column operating at 80.0 barg. The advancement of CO_2 absorption has greatly improved with the integration of auto-amine concentration monitoring and makeup mechanisms. By employing inline probes, the feedback control system consistently evaluates the electrical conductivity variables of the PZ+MDEA stream against the 700 µS/cm reference signal, enabling immediate and precise adjustments to the absorption parameters, selectively regulating the ratios of dry amine and water through three-way control valves to maintain the 40 – 45g/100ml stability for optimum CO_2 capture. This automation method at PZ+MDEA 43.34 g/100ml inlet concentration, 702.16 micro S/cm EC, 46.5^{o}C lean amine, and pH of 11.34 reduced the rich gas stream CO_2 of 20,104.77ppm to 258.51 ppm residue with an average performance of 98.72% and is poised to become a key aspect of sustainable industrial practices.

Keywords: *CO_2 capture; Advanced Process Control; Amine concentration monitoring and makeup; Piperazine-activated Methyl-di-ethanolamine.*

1.0 Introduction

In recent years, increasing carbon dioxide emissions have become a significant concern for environmental sustainability. One promising solution to mitigate these emissions is the optimization of CO_2 absorption using innovative technologies such as a selective makeup Advanced Process Control system (Fayruzov, Bel'kov, Kneller, & Torgashov, 2017), a refined approach designed to enhance the operational efficiency, PZ+MDEA (Ng, Lau, Chin, & Lim, 2023), and demineralized water blending ratio (Yuan *et al.*, 2022), and intelligent utilization of PZ+MDEA solvent to optimize and stabilize the process concentration and ultimately lead to an improved CO_2 absorption performance (Aghel *et al.*, 2022).

Resolving treated and compressed natural gas production with high CO_2 and off-spec NGL by utilizing electrical conductivity inline probes, PID Controller, and final control elements configured to enhance the overall performance and efficiency of the CO_2 mass transfer process and potentially moving towards a more sustainable future is vital due to potential pipeline corrosion and safety risks (Liang *et al.*, 2022). Off-spec NGL affects product quality, resulting in

economic losses and regulatory issues. Tackling these glitches enhances safety, environmental compliance, and system integrity.

2.0 Methodology

The original composition of the regenerative solvent MDEA + PZ consists of 94%w/w base amine methyl-di-ethanolamine and 6%w/w reactive amine Piperazine. This composition enables selective absorption of CO_2 from rich natural gas. The PZ+MDEA quality assurance test shows an average pH of 11.72, an average purity strength of 94.97%w/w, and a 6.6% water cut. The PZ+MDEA solvent has a relative density of 1.0432 and a boiling point range of 127 – 247°C ***(Table 1),*** making it suitable for efficient regenerations (Ma *et al.*, 2023). The demineralized water pH fluctuates from 11.23 to 4.23 and back to 11.50 ***(Table 2)*** affecting the optimal pH requirement for the PZ+MDEA blending process (Zhang *et al.*, 2021). Effective backwashing and unit regeneration sequences improve demi-water quality (Turan, 2023).

Table 01. PZ+MDEA commercial supply purity quality assurance tests before blending

PZ+MDEA Product	Appearance	Physical State	Odor	pH	PZ+MDEA Concentration	Relative Density	Initial Boiling Point	Boiling Point Range	Boiling Point @ 95% Recovery	Water Content	Solubility in Water
(Drum)	(Color)	(Solid or Viscous)	(Foul, Pungent, Amine)	(10% in aqueous medium)	(%)	(@ 25°C)	(°C)	(°C)	(°C)	(% Vol)	(Highly soluble, sparingly Soluble or insoluble)
1	Colorless	Viscous Liquid	Amine-like	11.62	93.75	1.0466	105	127.00 - 247.00	247	7	Completely miscible
2	Colorless	Viscous Liquid	Amine-like	11.76	94.90	1.0414	105	127.00 - 247.00	247	7	Completely miscible
3	Colorless	Viscous Liquid	Amine-like	11.78	94.66	1.0423	105	127.00 - 247.00	247	7	Completely miscible
4	Colorless	Viscous Liquid	Amine-like	11.75	95.85	1.0409	105	127.00 - 247.00	247	6	Completely miscible
5	Colorless	Viscous Liquid	Amine-like	11.74	92.99	1.0330	105	126.00 - 247.00	247	7	Completely miscible
6	Colorless	Viscous Liquid	Amine-like	11.70	95.85	1.0409	105	127.00 - 247.00	247	6	Completely miscible
7	Colorless	Viscous Liquid	Amine-like	11.71	95.81	1.0466	105	127.00 - 247.00	247	6	Completely miscible
8	Colorless	Viscous Liquid	Amine-like	11.65	95.83	1.0410	105	127.00 - 247.00	247	6	Completely miscible
9	Colorless	Viscous Liquid	Amine-like	11.77	94.85	1.0422	105	127.00 - 247.00	247	7	Completely miscible
10	Colorless	Viscous Liquid	Amine-like	11.76	94.95	1.0309	105	127.00 - 247.00	247	7	Completely miscible

Table 02. Demineralized water production quality assurance tests before blending

Observations	De-Mineralized Water Resin Bed					De-Mineralized Water Storage Unit				
	Demi Water Generation Resin Bed Unit-A					Demi Water Storage Tank				
	Operating Temperature (°C)	Operating Pressure (Barg)	pH	Conductivity @ 25 °C, (µ/cm)	Total Dissolved Solids (mg/l)	Operating Temperature (°C)	Operating Pressure (Barg)	pH	Conductivity @ 25 °C, (µ/cm)	Total Dissolved Solids (mg/l)
Day-1	138.0	2.40	**11.23**	**11.70**	5.85	138.0	2.40	**11.10**	**11.70**	5.85
Day-2	138.0	2.40	**11.10**	**9.20**	4.60	138.0	2.40	**11.00**	**10.20**	5.10
Day-3	138.0	2.40	**11.50**	**10.90**	5.45	138.0	2.40	**11.20**	**10.00**	5.00
Day-4	138.0	2.40	**11.20**	**9.80**	4.90	138.0	2.40	**11.10**	**9.60**	4.80
Day-5	138.0	2.40	**11.10**	**10.70**	5.35	138.0	2.40	**11.00**	**10.50**	5.25
Day-6	138.0	2.40	**8.53**	**11.50**	5.75	138.0	2.40	**9.53**	**11.40**	5.70
Day-7	138.0	2.40	**5.91**	**8.50**	4.25	138.0	2.40	**4.75**	**11.10**	5.55
Day-8	138.0	2.40	**5.11**	**11.60**	5.80	138.0	2.40	**5.26**	**8.40**	4.20
Day-9	138.0	2.40	**4.96**	**8.20**	4.10	138.0	2.40	**4.93**	**7.40**	3.70
Day-10	138.0	2.40	**4.87**	**9.90**	4.95	138.0	2.40	**4.71**	**8.60**	4.30

2.1. Piperazine-Activated Methyl-di-ethanolamine Stock Solution Dilution Equation

C_1 x V_1 = C_2 x V_2 (2.1)

Where:

C_1 = PZ+MDEA average stock concentration (initial concentration)

V_1 = PZ+MDEA average stock volume or blend (initial volume).

C_2 = PZ+MDEA new solution concentration (desired concentration)

V_2 = PZ+MDEA new solution volume (desired or final volume).

C_1 = 94.43%

V_1 = 1 drum or 210 litres

C_2 = 45 g/100 ml or 45%

V_2 =?

$= 94.43\% * 210Lts = 45\% * V_2$ (2.2)

$\frac{94.43\%*210Lts}{45\%} = V_2$ (2.3)

$V_2 = \frac{19{,}830.3}{45}$ (2.4)

$V_2 = 440.673\ Lts$ (2.5)

Therefore; free demineralized water volume = 440.673 – 210

$= 230.673\ Lts$ (2.6)

Dilution rate or ratio$= \frac{210}{230.67}$ = 1.0984 or 1.1 (2.7)

1 volume of PZ+MDEA blends mixed with 1.1 volume of demineralized water to yield a total volume of 2.1 or (210 + 230.67 Lts = 440.67). (2.8)

2.2.Optimum Piperazine-activated Methyl-di-ethanolamine (MDEA) Concentration

$$\frac{v}{v}\%\ concentration = \frac{Volume\ of\ solute\ g}{Volume\ of\ solution\ ml} * 100 \quad (2.9)$$

$$\frac{v}{v}\%\ concentration = \frac{94.43\ g}{210*1000} * 100 \quad (2.10)$$

$$\frac{v}{v}\%\ concentration = \frac{94.43}{210} * 100 \quad (2.11)$$

$$\frac{v}{v}\%\ concentration = 0.4496666 * 100 \quad (2.12)$$

$$\frac{v}{v}\%\ concentration = 44.967\ \text{Or}\ 45.0 \quad (2.13)$$

2.3.Selective Makeup Advanced Process Control

The selective makeup Advanced Process Control (APC) aims to optimize and stabilize the amine process concentration, CO_2 mass transfer, and absorption ***(Figure 1)***. By forecasting PZ+MDEA electrical conductivity and concentrations optimum ranges and desired value, the kinetic model through APC PID controller facilitates and optimizes Absorption Column-A/B operating parameters, improving gas recovery and reliability in chemical processes.

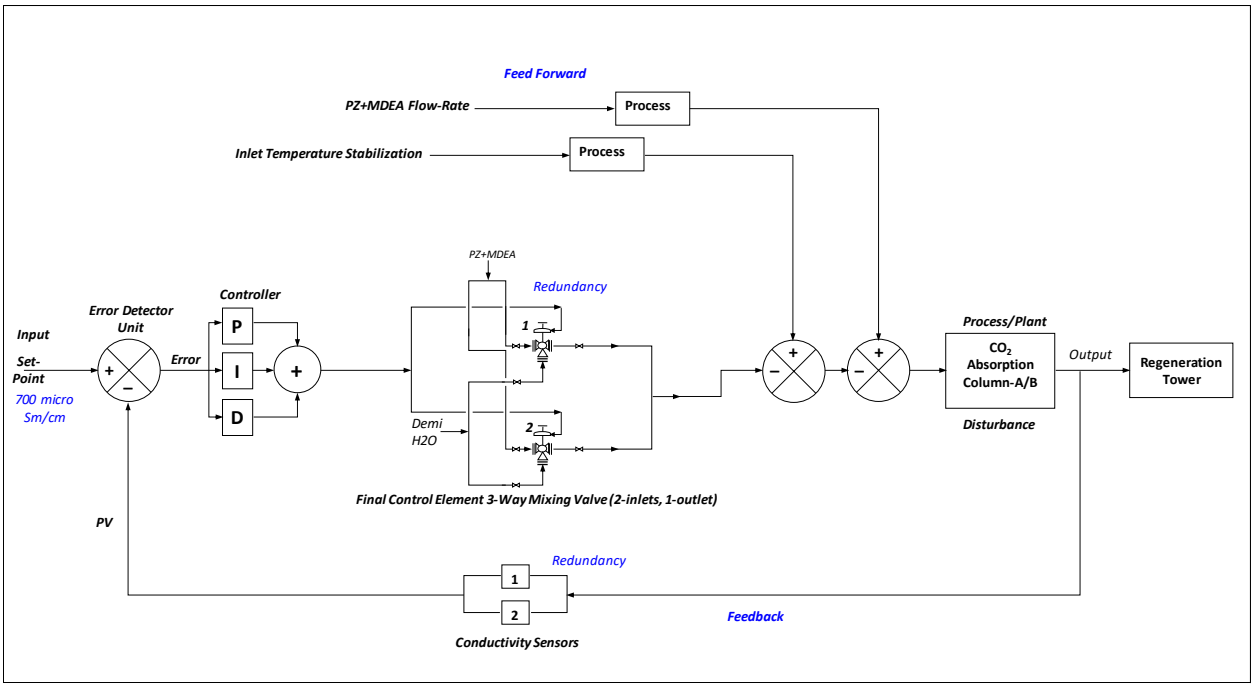

Figure 01. Selective PZ+MDEA and Demi-water makeup Advanced Process Control

2.4.Flow and Consistency Self-Regulating Process Control Loop Manual Tuning Sequence

Close Visual Inspection of the final control element and control system ascertained design architecture, composition, and conditions of the parts and make. The bump test to understand the cause-and-effect relationship between the control loop Process Variable (PV) and Controller Output (CO) by introducing a change in the CO to observe the PV response and process dynamics through a gradual step motion, the pulse test was preferred and utilized. The simple 1st order model helped to identify the relationship between the controller output change, the process variable response, and how much it takes to move and get there for a given change.

Process Gain: $K_p = \frac{\Delta PV}{\Delta Output}$ (2.14)

Time Constant: $\tau_p \cong \frac{\Delta Time}{4}$ (2.15)

Tuning:

PID Algorithms classes:

i. Standard: $K_C \left(1 + \frac{1}{T_1 S} + T_D S\right)$ (2.16)

ii. Parallel: $K_p + \frac{K_I}{S} + K_D S$ (2.17)

iii. Classical: $K_c \left(1 + \frac{1}{T_1 S}\right)(1 + T_D S)$ (2.18)

Where:

T = Time, K_C = Controller gain, K_P = Proportional band, T_D = Derivation time

Tune Rule: There are 1st and 2nd order response:

The 1st-order closed-loop response: $K_{cl} = \frac{\Delta PV}{\Delta SP} = 1$ (2.19)

$K_C = \frac{1}{K_P \ \tau_{Ratio}}$ (2.20)

$T_I = \tau_P$ (2.21)

$T_D = \emptyset$ (2.22)

τ_{Ratio} Defines speed

$\tau_{Ratio} = \frac{\tau_{cl}}{\tau_p}$ (2.23)

Where:

K_{cl} = closed loop gain, T_I = Integral Time, T_D = Derivative Time, K_c = Control gain, K_P = Process gain, τ_P = Process Time and τ = Defines speed. τ_{cl} = Closed loop time constant, τ_P Open loop process time constant.

2.5. Demineralized Water and PZ-activated MDEA Stock Pre-mixing

A maximum of 245.7 liters of demineralized water was added at a dilution ratio of 1:1.1 to achieve a 441 liters solution through the three-way valve, after mixing, the lean PZ+MDEA blend at an average pH of 11.36 was delivered through the centrifugal pumps into the top tray of the parallel operating Absorption Columns at about 80.0 barg and an average solvent inlet temperature of 46.43°C ***(Figure 1, Table 4)***.

C_1 = PZ+MDEA average stock concentration (initial concentration)

V_1 = PZ+MDEA stock volume or blend (initial volume); 1 drum or 210 litres

C_1 = 94.43% containing: $\frac{94.43}{100} = 0.9443$ (2.24)

C_1 containing = 210 * 0.9443 (2.25)

C_1 containing = 198.30 Litres of pure PZ+MDEA blend (2.26)

The volume of demineralized water required for mixing:

$$= (100 - 45) * \frac{\left(\frac{94.43}{100}\right)}{\left(\frac{100-94.43}{100}\right)} \quad (2.27)$$

$$= 55 * \left(\frac{0.9443}{0.0557}\right) \quad (2.28)$$

= 55 * 16.9533 (2.29)

= 932.432 ml (2.30)

932.43 = demineralized water must be added into the 45g/100 ml PZ+MDEA concentration to obtain 1 liter or 1,000.0 ml solution.

2.6. PZ Activated MDEA and Demineralized Water Make-up Automation

The inline sensor provides real-time monitoring of fluctuating PZ+MDEA electrical conductivity variations and process variable (PV) outlet of the Absorption Column using high-accuracy Alternating Current measurement technology and feedback to the proportional-integral-derivative (PID) controller. Selective three-way mixing valves makeup system is a direct action (DA) air-to-close system that responds to fluctuations in conductivity, concentration, and pH; facilitates the precise adjustment of solvent 1:1.1 mixing ratios based on the deviation of the process variable from the control set-point, pre-mixed and discharged, automatically replenishing the depleted amine solution with fresh blend, stabilizing PZ+MDEA concentration, and maintain an optimal CO_2 capturing and absorption capacity ***(Figure 1).***

PID signal effectively controls the throttling valves, enabling accurate adjustment of the Piperazine-activated Methyl-di-ethanolamine or demineralized water supply on a balanced ratio. For enhanced availability and reliability of data analysis, the two in-line monitoring electrical conductivity sensors deployed at the Absorption Column and Regeneration tower PZ+MDEA inlet study points are required to function constantly. The temporary failure of one probe will transfer the monitoring role to the available alternative until corrective maintenance is effected to restore bi-monitoring functionality ***(Figure 1)***.

The control loop's electrical conductivity Process Variable (PV) fluctuates around 700 micro S/cm Reference Signal, by -64% to 129%, which is within the optimal 40 – 45 g/100ml PZ+MDEA solution concentration, ensuring at least 99% CO_2 absorption and a residual CO_2 concentration below 250 ppm in the sweetened natural gas stream. The electrical conductivity control set-point of 700 µS/cm signifies effective ionization and promotes ionic interactions that aid CO_2 capture in gas treatment ***(Figure 2)***.

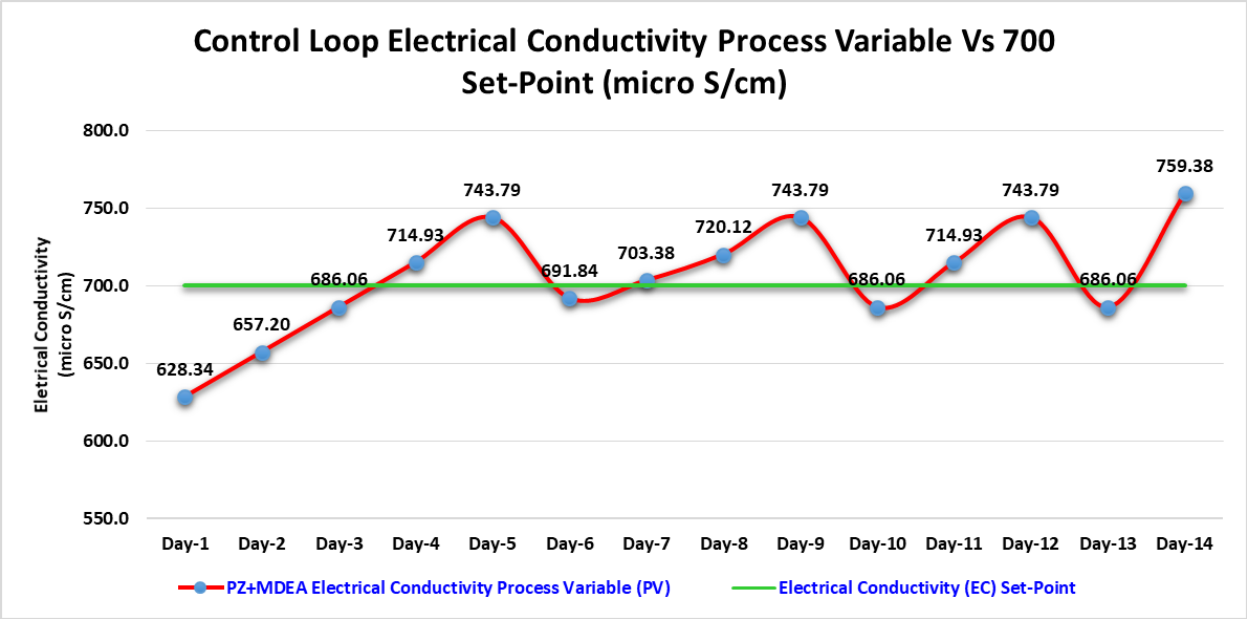

Figure 02. Control loop set-point and electrical conductivity process variations

3.0. Results and Discussion

When the electrical conductivity process variable (PV) is within the 686 – 700 micro S/cm range, the proportional-integral-derivative (PID) algorithm controller automatically sends signal and adjusts the inlet openings of the three-way valve to restore the desired conductivity (PZ+MDEA concentration) to the optimum value, the 3-way valve inlet port-A fed by the dry PZ+MDEA pump attains about 46% optimum and maximum opening, the port-B opening (demi-water) reaches 54% for an average mixture of 1:1.1 ratio, and exit through discharge port AB. Inlet port-B gradually closes when 703 to 760 micro S/cm electrical conductivity PV exceeds the set-point (indicating

concentration reduction) to reduce the inflow of demi-water, as port-A is still open at 46% to admit and sustain PZ+MDEA concentration ***(Figure 1&3)***.

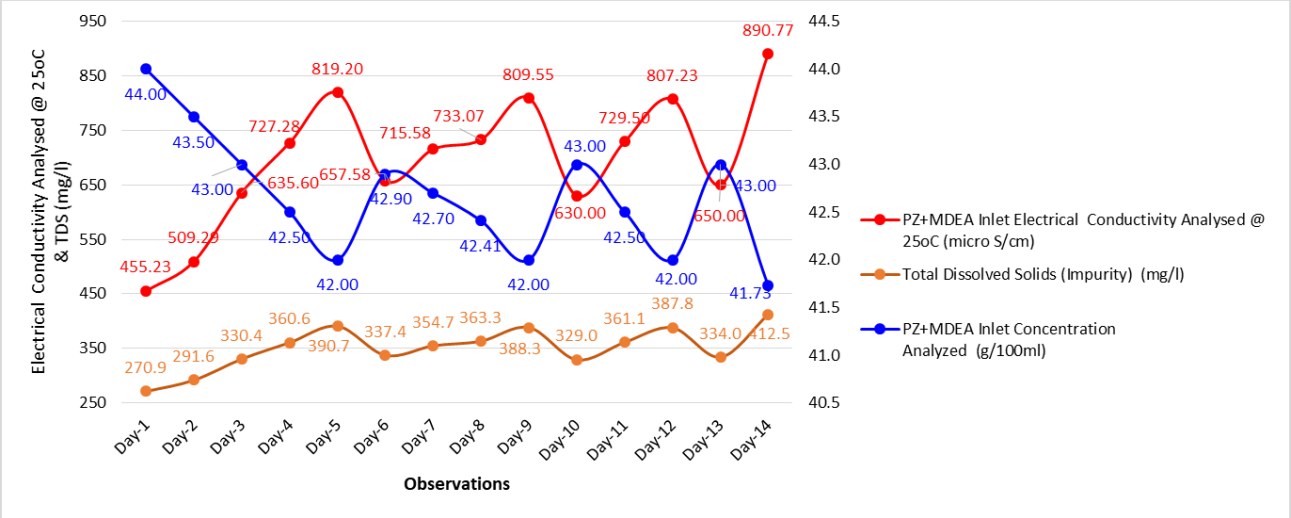

Figure 03. Optimized PZ+MDEA electrical conductivity/concentration/TDS relationship

The optimized EC varies from 455.23 micro S/cm to 890.77, TDS from 270.9 mg/l to 412.5 mg/l, and negatively correlated PZ+MDEA strength from 40 g/100ml to 45g/100ml. The optimized process variables and the affected range include an operating pressure of 77 – 80barg, temperature range of 45 – 65ºC, PZ+MDEA concentration of 40 – 45 g/100ml, experimental data electrical conductivity of 450 – 900 micro S/cm, kinetic model electrical conductivity range of 600 – 800 micro S/cm, total dissolved solids of 250 – 450 mg/l and pH value of 8.0 – 11.8 ***(Figure 3, Table 3&4)***.

A match of +7.843 micro S/cm between predicted and experimental conductivity indicates the kinetic model effectively represents the gas sweetening process in the absorption column. This agreement shows the model's reliability for optimization, reflecting actual system conditions, which is vital for enhancing efficiency, ensuring optimal operation, and reducing costs in sweetening ***(Table -3)***.

Absorption Column-A/B 77 – 80 Barg Operating Pressure Optimization Range

Operating Absorption Columns at 77 – 80 Barg high pressure range, can significantly enhance CO_2 mass transfer and absorption efficiency. The increased pressure improves the solubility of CO_2 in the absorbing liquid, leading to enhanced interaction between the gas and liquid phases (Huang *et al.*, 2019). This optimizes the overall performance of absorption processes, particularly in technologies focusing on CO_2 capture. It's also noted that parameters such as liquid flow rates (131.1 Tons/Hrs) and 45ºC – 65ºC temperature range obtained through this study considerably affect mass transfer coefficients, which are critical for effective absorption in these high-pressure conditions ***(Table -4)***.

Table 03. Absorption Column-A/B inlet stream analyzed and predicted electrical conductivity

Observations (Days)	Absorption Column PZ+MDEA Inlet Concentration Analyzed (g/100ml)	Unit-A/B PZ+MDEA Inlet Average Electrical Conductivity Analysed @ 25oC, (micro S/cm)	Unit-A/B PZ+MDEA Inlet Average Electrical Conductivity Model Prediction, (micro S/cm)	Control Loop PZ+MDEA Eletrical Conductivity Set-Point (micro S/cm)	Unit-A/B Lean PZ+MDEA Electrical Conductivity Differential (Δ micro S/cm)
Day-1	44.00	455.23	628.34	700.0	173.109
Day-2	43.50	509.29	657.20	700.0	147.912
Day-3	43.00	635.60	686.06	700.0	50.465
Day-4	42.50	727.28	714.93	700.0	-12.352
Day-5	42.00	819.20	743.79	700.0	-75.409
Day-6	42.90	657.58	691.84	700.0	34.257
Day-7	42.70	715.58	703.38	700.0	-12.197
Day-8	42.41	733.07	720.12	700.0	-12.947
Day-9	42.00	809.55	743.79	700.0	-65.759
Day-10	43.00	630.00	686.06	700.0	56.065
Day-11	42.50	729.50	714.93	700.0	-14.572
Day-12	42.00	807.23	743.79	700.0	-63.439
Day-13	43.00	650.00	686.06	700.0	36.065
Day-14	41.73	890.77	759.38	700.0	-131.393
	42.66	**697.85**	**705.69**		**7.843**

Table 04. Absorption Column-A/B optimized process variable ranges

Observations (Days)	Operating Pressure (Barg)		Operating Temperature (°C)		PZ+MDEA Inlet Concentration Analyzed (g/100ml)	PZ+MDEA Inlet Electrical Conductivity Analysed @ 25°C (micro S/cm)	PZ+MDEA Inlet Electrical Conductivity Model Prediction	PZ+MDEA Inlet Electrical Conductivity - Average	Total Dissolved Solids (Impurity) (mg/l)	pH	
Day-1	(Inlet)	(Outlet)	(Inlet)	(Outlet)	(g/100ml)	(micro S/cm)	(micro S/cm)	(micro S/cm)	(mg/l)	(Inlet)	(Outlet)
Day-2	77.0	77.0	51	55	44.00	455.23	628.34	541.78	270.9	11.23	8.79
Day-3	78.0	78.0	50	54	43.50	509.29	657.20	583.25	291.6	11.11	8.84
Day-4	78.0	78.0	50	55	43.00	635.60	686.06	660.83	330.4	11.24	8.86
Day-5	79.0	79.0	45	52	42.50	727.28	714.93	721.10	360.6	11.33	8.92
Day-6	79.0	79.0	45	55	42.00	819.20	743.79	781.50	390.7	11.19	9.10
Day-7	78.0	78.0	45	53	42.90	657.58	691.84	674.71	337.4	11.23	8.87
Day-8	78.0	78.0	45	55	42.70	715.58	703.38	709.48	354.7	11.44	8.90
Day-9	79.0	79.0	52	57	42.41	733.07	720.12	726.60	363.3	11.54	9.00
Day-10	79.0	79.0	54	58	42.00	809.55	743.79	776.67	388.3	11.71	9.14
Day-11	79.0	79.0	50	55	43.00	630.00	686.06	658.03	329.0	11.42	8.86
Day-12	78.0	78.0	55	62	42.50	729.50	714.93	722.21	361.1	11.22	8.92
Day-13	79.0	79.0	54	59	42.00	807.23	743.79	775.51	387.8	11.29	9.16
Day-14	79.0	79.0	54	59	43.00	650.00	686.06	668.03	334.0	11.4	8.86
	79.0	79.0	53	58	41.73	890.77	759.38	825.07	412.5	11.25	9.18
Average:	**78.5**	**78.5**	**50.2**	**56.2**	**42.66**	**697.85**	**705.69**	**701.77**	**350.89**	**11.33**	**8.96**
Range:	**(77 - 80) Barg**		**(45 - 65) °C**		**(40 -45) g/100ml**	**(450 - 900) micro S/cm**	**(600 - 800) micro S/cm**	**(500 - 850) micro S/cm**	**(250 - 450) mg/l**	**(8.0 - 11.8)**	

Absorption Column-A/B 45ºC – 65ºC Operating Temperature Optimization Range

Operating temperatures within the 45°C to 65°C range observed during this study can enhance mass transfer rates and absorption efficiency ***(Table -4)***, allowing for effective CO_2 capture

without significant detriment to absorption (Milshtein *et al.*, 2017). The significance lies in balancing energy costs and absorption performance, as higher temperatures may enhance CO_2 solubility and reaction kinetics but could also increase operational expenses. Research indicates that variations in temperature between 25°C and 65°C have minimal impact on pollutant removal efficiency, including CO_2 absorption (Hanifa *et al.*, 2023).

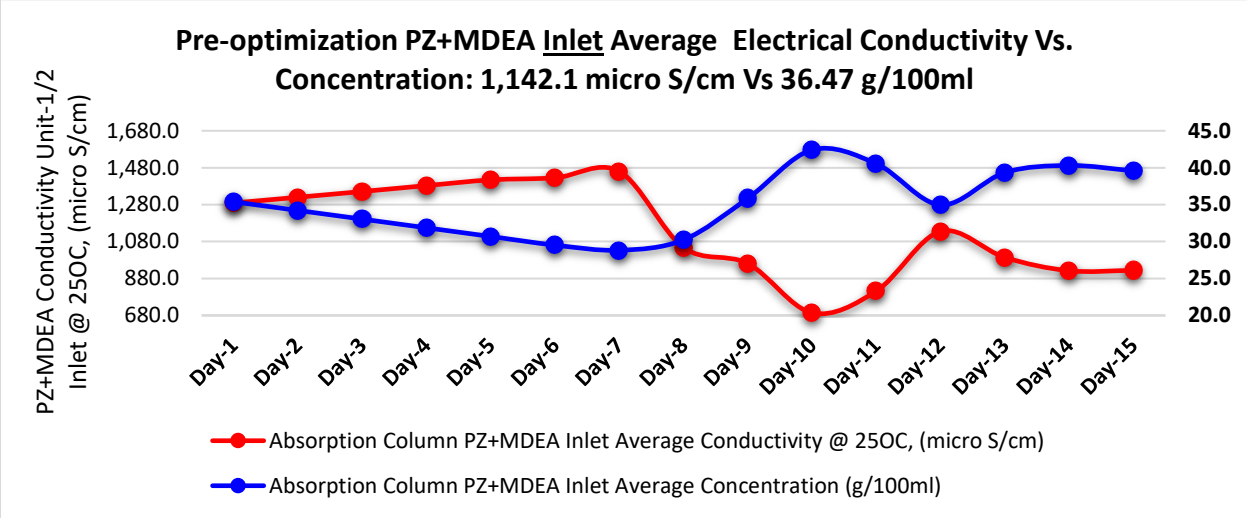

Figure 04. Absorption Column-A/B pre-optimization PZ+MDEA inlet conductivity Vs concentration –average

Absorption Column-A/B 40 – 45 g/100ml PZ+MDEA Optimal Concentration Range

Absorption Column-A/B 40 – 45 g/100ml PZ+MDEA inlet stream experimentally validated optimal concentration range typically indicates a balanced approach to maximizing CO_2 absorption efficiency. Based on a strong negative correlation and R2 of 0.9491 between Piperazine-activated Methyl-di-Ethanolamine electrical conductivity and concentration, the average inlet stream concentration improved to 42.66 g/100ml and stabilized outlet concentration to 41.0 g/100ml ***(Table -4, Figure 5&6)***. The electrical conductivities reacted to CO_2 absorption and concentration depletion in the opposite direction. The significance of optimizing the PZ+MDEA concentration lies in its impact on the mass transfer properties and absorption rates of CO_2, as a higher concentration can enhance the reactive surface area and increase the absorption capacity (Cao *et al.*, 2021). However, excessive concentrations may lead to operational issues and increased costs.

Absorption Column-A/B 450 – 900 micro S/cm PZ+MDEA Inlet Stream Optimal Electrical Conductivity Range

The results indicate that the electrical conductivity range of 450 – 900 µS/cm for the Absorption Column using a 6%w/w PZ and 94%w/w MDEA blend is significant as it reflects the ionic strength and the effectiveness of the CO_2 absorption process ***(Table 1&4)***. Higher electrical conductivity inversely correlates with increased ion concentration based on research pre-optimization R = -0.9742759, R^2 = 0.9491 and validated by post-optimization R = -0.99244776 and R^2 = 0.985, which enhances mass transfer performance in CO_2 absorption (Kuang *et al.*, 2023). The optimization of PZ and MDEA concentrations facilitates improved absorption rates and solubility of CO_2, which is crucial for efficient carbon capture technologies.

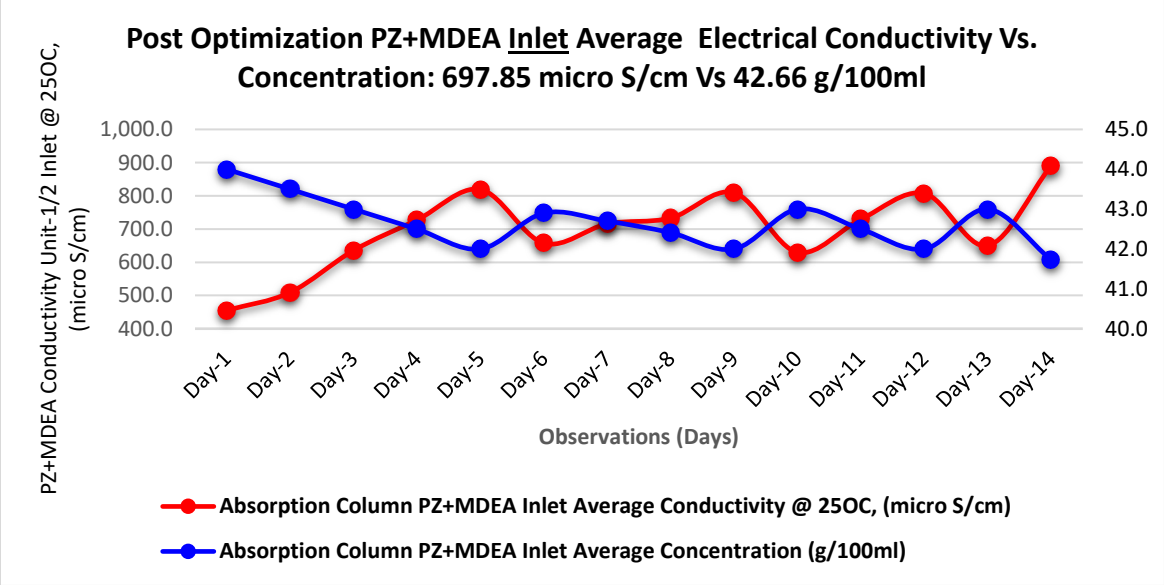

Figure 05. Absorption Column-A/B post-optimization PZ+MDEA inlet conductivity Vs concentration -average

Absorption Column-A/B 600 – 800 micro S/cm PZ+MDEA Inlet Stream Optimized Kinetic Model Electrical Conductivity Range

The Absorption Column-A/B with a PZ+MDEA inlet stream electrical conductivity kinetic model range of 600-800 µS/cm validated by detailed experimental data ***(Table 4)***, suggests effective ionic interaction and mass transfer properties, which are crucial for enhancing CO_2 absorption efficiency. The significance of optimizing the conductivity lies in its correlation with the mass transfer rate and energy consumption during CO_2 capture (Pan, Wang, Jin, & Cai, 2022). Higher conductivity can often lead to better ion mobility and interactions, improving the overall absorption kinetics and reducing the energy needed for CO_2 removal during regeneration, as

supported by recent studies showing improved gas absorption characteristics with enhanced ionic solutions (Ye, Williams, & Franklin, 2022).

Absorption Column-A/B 250 – 450 mg/l PZ+MDEA Inlet Stream Optimal Total Dissolved Solids Range

The results indicate that total dissolved solids (TDS) concentration in the Absorption Column-A/B utilizing PZ+MDEA solvent is critical for optimizing CO_2 capture efficiency (Hossain *et al.*, 2023). Specific concentrations like 250 to 450 mg/l can impact mass transfer rates ***(Table 4)***, where a concentration of 5 m PZ/2.3 m AMP has shown higher mass transfer rates compared to 8 m PZ at rich loading (Milshtein *et al.*, 2017). Lower alkalinity can reduce CO_2 capacity, emphasizing the need to balance TDS for better absorption performance (Sonnichsen *et al.*, 2023). Thus, optimizing TDS can significantly enhance CO_2 mass transfer and overall absorption efficiency (Hossain *et al.*, 2023).

Absorption Column-A/B PZ+MDEA Optimal pH 8.0 – 11.8 Range

The experimental data pH range of 8.0 to 11.8 ***(Table 4)*** in an Absorption Column-A/B using Piperazine (PZ) activated Methyl-di-ethanolamine (MDEA) blend is essential for CO_2 absorption (Ratman *et al.*, 2010). In this optimized range, the effectiveness of CO_2 capture can be enhanced due to the optimal balance between the PZ+MDEA concentration and the pH, which influences the ionization states of the amines. Higher pH levels generally increase the concentration of free amine species available for CO_2 absorption, thus improving mass transfer and absorption efficiency (Abdel-azim, 2011). However, excessively high pH values may also lead to complications such as increased solvent degradation or the formation of other chemical species that may not be conducive to efficient absorption (Moser, *et al.*, 2023). Maintaining a specific pH in the 8.0 to 11.8 range between the inlet and outlet stream maximizes CO_2 absorption while minimizing operational issues (Kumar, *et al.*, 2023).

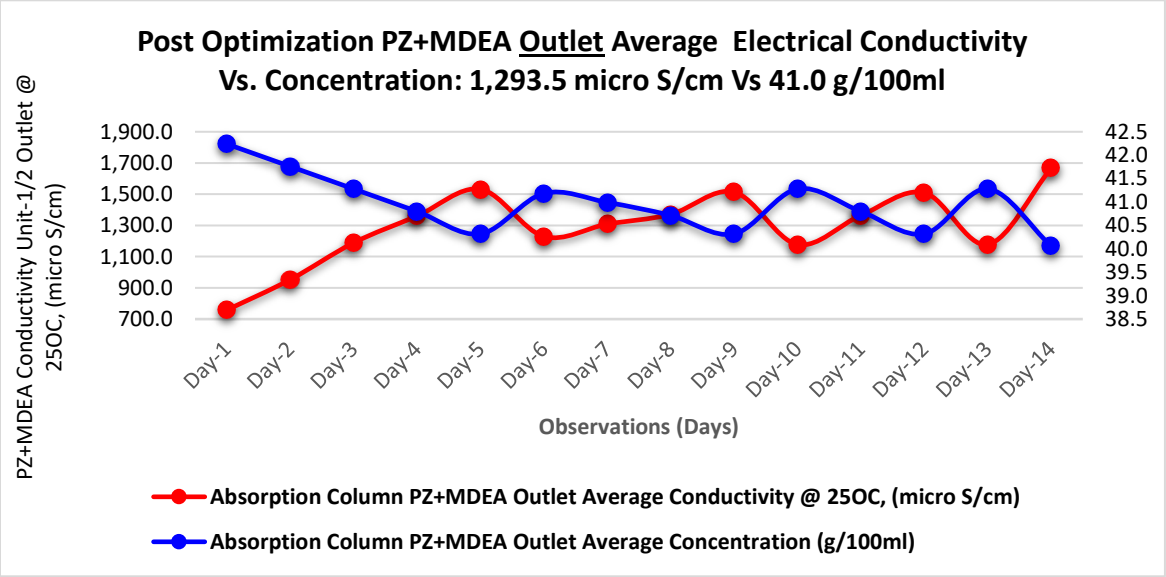

Figure 06. Absorption Column-A/B post optimization PZ+MDEA outlet conductivity Vs concentration -average

Validating the PZ+MDEA concentration and conductivity from discrete samples alongside integrated results ensures the accuracy and reliability of the gas-treating solvent's performance. This confirmation introduces confidence in the effectiveness of acid gas treatment and facilitates the optimization of unit operational parameters to enhance gas sweetening efficiency. The post-optimization Absorption Column-A/B PZ+MDEA solution inlet and outlet stream composite sampling and validation assessment shows that the pH levels are within the optimal range of 8.0 – 11.8 ***(Table 4)***. This indicates process stability and optimum mass transfer of acid gas CO_2 from the rich natural gas inlet stream into the lean PZ+MDEA absorbent (Kittel *et al.*, 2023).

The integrated sampling results before and after optimization showed consistency and repeatability with the discrete single samples collected from Absorption Column-A and Unit-B inlet streams. The concentration assessment indicated an average subsequent outcome of 42.66 g/100ml, representing an increase from the previous average of 36.47 g/100ml ***(Figure 4&5)*** due to the optimized control system (Pershin *et al.*, 2023).

Unit-A sweetened natural gas outlet stream showed improved calorific values after reducing the CO_2 content from 2.3953 Mol% to 0.16733 Mol%. The combustion energy and heating value output were higher at a reduced CO_2 composition and higher Wobbe index. Unit-B sweetened natural gas outlet stream showed improved calorific values and a higher Wobbe Index after scrubbing the CO_2 content from 2.3953 Mol% to 0.16733 Mol%. The gas flow's combustion energy and heating value will be higher than the inlet stream-rich gas ***(Figure 7&8)***.

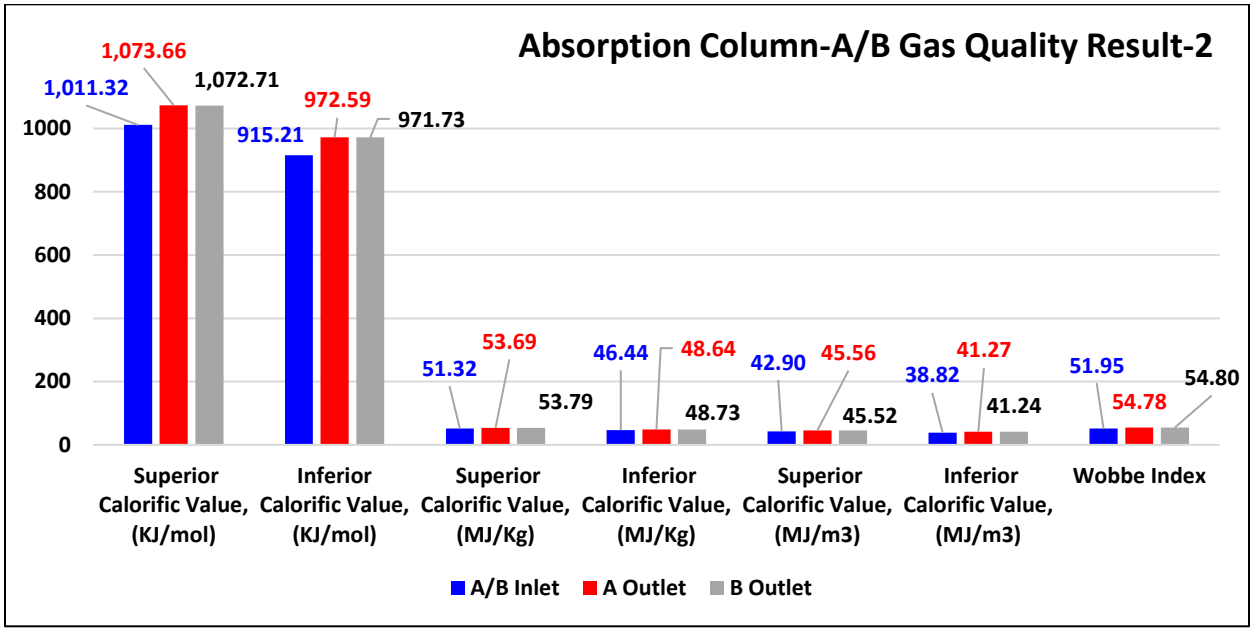

Figure 07. Absorption Column-A/B natural gas quality result

The value of Absorption Column-treated natural gas with a Wobbe index of 55 or higher lies in its superior combustion efficiency and interchangeability (Wang *et al.*, 2022). A higher Wobbe index indicates better energy delivery for industrial and residential use ***(Figure 7)***, while greater calorific values signify more energy per unit, enhancing fuel efficiency. This optimizes energy use, cuts emissions, and boosts efficiency in energy generation.

The effective synergy of three independent and complementary control loops is essential for optimizing the mass transfer of CO_2 from the rich natural gas stream to the lean PZ+MDEA solution: The main PZ+MDEA circulation pump ensures efficient absorbent liquid columns and contact surface while the forced draft heat exchangers maintain the required temperature of the PZ+MDEA inlet stream. Additionally, the retrofit selective make-up control system optimizes and stabilizes the concentration of the PZ+MDEA ***(Figure 1)***.

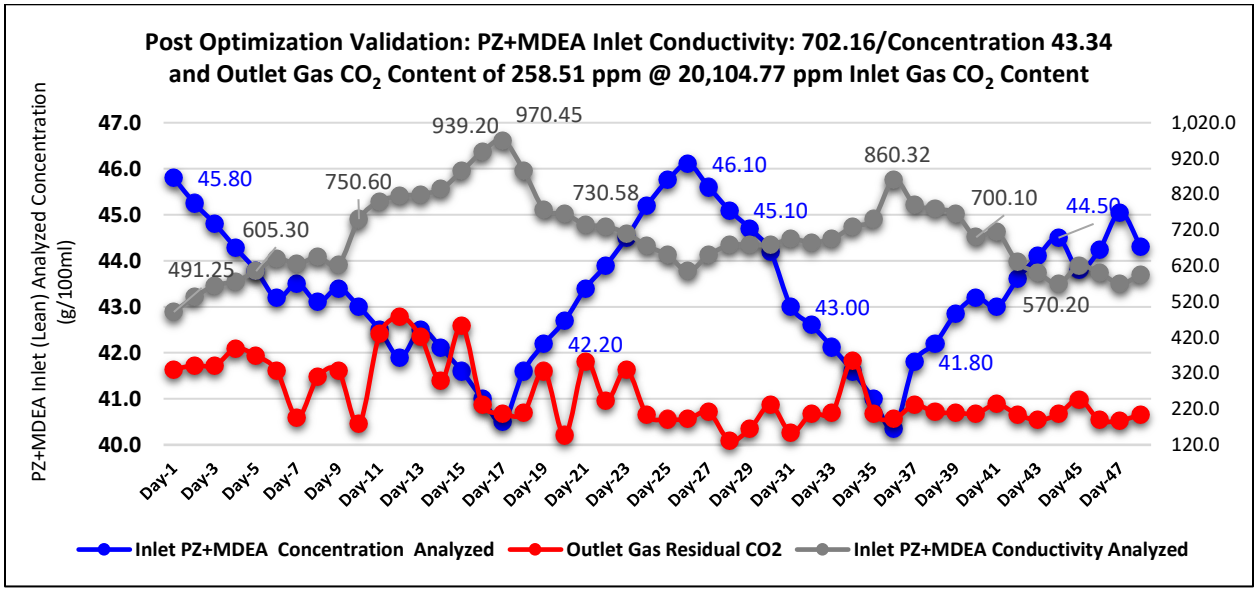

Figure 08. Absorption Column-A/B extensive experimental data validations

4.0. Post-optimization Validation

After a post-optimization 15-day assessment and subsequent 48-day validation of Absorption Column-A/B operating parameters ***(Figure 8)***, the inlet stream temperature decreased to 46.5^{o}C from 48.30^{o}C, and the outlet stream temperature varied to 55.5^{o}C from 54.60^{o}C. This change is due to CO_2 mass transfer which increased CO_2 concentration in the exit amine.

The experimental findings validations: at an average Absorption Column-A/B natural gas inlet stream CO_2 content of 20,104.77 ppm, PZ+MDEA inlet stream solution concentration of 43.34g/100ml, and electrical conductivity of 702.16 micro S/cm, the sweet gas outlet stream residual CO_2 content of 258.51 ppm, resulted in a performance efficiency of 98.72% ***(Figure 8)***.

The results showed that the treated gas outlet residual CO_2 content reduced to 0.0316 mol.% (258.51 ppm) at a PZ+MDEA outlet temperature of 55.5^{o}C and pH of 8.99, confirming an average performance of 98.72% ***(Figure 8)***.

5.0. Selective Automation Control System Practical Limitations

The interdependency of the control system in-line electrical conductivity probes, transmitters, *Proportional – Integral – Derivative* (PID) Controller and logic processor, input/output transducers (current-to-pneumatic converter), three-way valve final control mechanism, PZ+MDEA ***(Figure 1)***, and demineralized water auxiliary pumps, meant a failure in one component might lead to suboptimal performance or complete failure of the gas sweetening process (Cheng, *et al.*, 2022), thus the need for redundant and robust design with operational oversight. 30% of the CO_2-rich PZ+MDEA slip-stream from the Absorption Column-A/B flows through the activated carbon filter unit. There is a risk of failure beyond the scheduled maintenance, which may interfere with the quality and monitoring of PZ+MDEA.

The dry PZ+MDEA amine solution storage tank has a usage autonomy of 7 to 47 days based on fill-up volume. It's important to maintain the fill level between minimum and maximum for operational efficiency, safety, and cost management, a full tank ensures adequate absorbent for CO_2 absorption, while a lower fill level helps manage space and prevents degradation or contamination. Balancing operational readiness with solution integrity is vital for performance and safety.

The estimated depletion rate of demineralized water is 805.2 liters per day, based on an optimal circulation rate of 134,200.0 liters per hour. The storage tank capacity of 60,000.0 liters allows for 13 to 67 days of autonomy, depending on the fill-up volume. The water depletes faster when the storage percentage is closer to 20% and declines to the 5% Tank Dead Volume limit in 13 days. The demineralized water is less dense, generated internally, and stored in a high-density polyethylene (HDPE) Plastic coated tank with fewer contaminants.

The rich natural gas mixture volatile components, the absorbed CO_2, and vaporized CO_2 from the desorption unit are processed through controlled steps, then flared or dispersed into the atmosphere. This CO_2 compound could have been utilized as gas feedstock for carbon capture and sequestration systems.

6.0. Conclusion

The experimental findings demonstrate that with a natural gas inlet stream CO_2 content of 20,104.77 ppm and a PZ+MDEA concentration of 43.34g/100ml, alongside an electrical conductivity of 702.16 µS/cm, the absorption column achieved a sweet gas outlet residual CO_2 content of 258.51 ppm, this resulted in performance efficiency of 98.72%, indicating highly effective CO_2 removal capability during the absorption process ***(Figure 8)***.

It's important to control PZ+MDEA concentration from rising above 50 g/100 ml ***(Figure 8)***, as higher limits may increase the viscosity and surface tension thus inhibiting CO_2 mass transfer through the aqueous layers (Deshko, Bilous, & Hetmanchuk, 2023). The 46.5ºC to 55.5ºC exothermic change between the inlet and outlet streams in the PZ+MDEA absorption process shows that heat is released during CO_2 absorption, enhancing the column's efficiency and driving higher CO_2 removal rates (Takahashi *et al.,* 2020). Additionally, a drop in amine outlet pH from 11.34 on average to 8.99 indicates changes in loading capacity and acid gas absorption (Triki, Herrero, Jiménez-Colmenero, & Ruiz-Capillas, 2018). Optimizing these factors can improve natural gas sweetening by maximizing CO_2 removal and minimizing energy use (Alardhi, Al-Jadir, Hasan, Jaber, & Al Saedi, 2023).

The three-way control valve system is not a replacement for the main amine circulation pumps, it automatically adjusts the delivery of lean amine blend relative to the 700 micro S/cm reference signal ***(Figure 1&2)*** to maintain the optimal concentration in the circulation loop. Optimizing a gas-sweetening absorption column involves adjusting factors like high pressure, amine concentration, conductivity, total dissolved solids, and pH to enhance efficiency and reduce energy use (Chen *et al.,* 2021). Higher pressures improve gas absorption, while optimal amine

concentrations effectively remove CO_2 (Prusti *et al.*, 2023). Real-time monitoring of pH and conductivity maintains solvent performance and minimizes undesirable byproducts, ultimately lowering operational costs and boosting system performance (Jeon *et al.*, 2014; Huang *et al.*, 2023).

The automated amine selective makeup control system ***(Figure 1)*** is innovative for sustaining high CO_2 absorption rates (Boulmal, Rivera-Tinoco, & Bouallou, 2018), improving overall process efficiency (Tollefson & Gulbrandson, 2023), optimizing amine usage (Bulan & Oz, 2021), reducing wastages, and lowering energy requirements (Slameršak, Kallis, & O'Neill, 2022) and operational costs. The emphasis on intelligent amine control and operational reliability highlights the industry's transition towards more sustainable and energy-efficient carbon capture solutions (Shen *et al.*, 2023), utilizing advanced technology to tackle the complexities of climate change (Intergovernmental Panel on Climate Change, 2023).

Pursuing advancement in gas-sweetening technology emphasizes the ever-evolving landscape of academic research in environmental engineering, focusing on mitigating greenhouse gas effects and improving industrial operations' sustainability (Alardhi *et al.*, 2023). Despite innovations, gaps still exist in optimizing energy consumption, amine degradation, and handling of waste products. Integrating these technologies seamlessly under various industrial conditions is also a challenge.

References

1. Abdel-azim, A. (2011). Fundamentals of Heat and Mass Transfer.
2. Aghel, B., Janati, S., Alobaid, F., Almoslh, A., & Epple, B. (2022). Application of Nanofluids in CO_2 Absorption: A Review. Applied Sciences.
3. Alardhi, S., Al-Jadir, T. M., Hasan, A., Jaber, A., & Al Saedi, L. M. (2023). Design of Artificial Neural Network for Prediction of Hydrogen Sulfide and Carbon Dioxide Concentrations in a Natural Gas Sweetening Plant. Ecological Engineering & Environmental Technology.
4. Alardhi, S., Al-Jadir, T. M., Hasan, A., Jaber, A., & Al Saedi, L. M. (2023). Design of Artificial Neural Network for Prediction of Hydrogen Sulfide and Carbon Dioxide Concentrations in a Natural Gas Sweetening Plant. Ecological Engineering & Environmental Technology.
5. Boulmal, N., Rivera-Tinoco, R., & Bouallou, C. (2018). Experimental assessment of CO_2 absorption rates for aqueous solutions of hexylamine, dimethylcyclohexylamine and their blends.
6. Cao, Y., Rehman, Z., Ghasem, N., Al-Marzouqi, M., Abdullatif, N., Nakhjiri, A. T., ... Shirazian, S. (2021). Intensification of CO_2 absorption using MDEA-based nanofluid in a hollow fibre membrane contactor. Scientific Reports, 11.
7. Chen, K., Wang, N. N., Yin, Q., Gu, Y. H., Jiang, K., Tu, Z., ... Cheng, J. (2021). Double Superconducting Dome and Triple Enhancement of Tc in the Kagome Superconductor CsV3Sb5 under High Pressure. Physical Review Letters, 126(24), 247001.
8. Cheng, Q., Zhang, L., Dai, J., Tang, W., Ke, J., Liu, S., Liang, J., Jin, S., & Cui, T. (2022). Reconfigurable Intelligent Surfaces: Simplified-Architecture Transmitters—From Theory

to Implementations. Proceedings of the IEEE, 110, 1266-1289. doi: 10.1109/JPROC.2022.3158479

9. Deshko, V., Bilous, I., & Hetmanchuk, H. (2023). Research of air exchange in the apartment on the basis of experimental determination of CO_2 mass transfer. Energy and automation.
10. Fayruzov, D. K., Bel'kov, Y. N., Kneller, D. V., & Torgashov, A. (2017). Advanced process control system for a crude distillation unit. A case study. Automation and Remote Control.
11. Hanifa, M., Agarwal, R., Sharma, U., Thapliyal, P., & Singh, L. (2023). A review on CO_2 capture and sequestration in the construction industry: Emerging approaches and commercialised technologies. Journal of CO_2 Utilization.
12. Hossain, M. S., Kumar, D., Azad, M. A. S., Azam, S. M. S., Amin, M. S. A., & Mozumder, M. S. I. (2023). A Comparative Study on CO_2 Capture Efficiency Using Single and Blended Solvent. Process Integration and Optimization for Sustainability.
13. Huang, G., Du, S., & Wang, D. (2023). GNSS techniques for real-time monitoring of landslides: a review. Satellite Navigation, 4, 1-10.
14. Huang, W., Zheng, D., Xie, H., Li, Y., & Wu, W. (2019). Hybrid physical-chemical absorption process for carbon capture with strategy of high-pressure absorption/medium-pressure desorption. Applied Energy.
15. IM Pershin, EG Papush, TV Kukharova, VA Utkin Water, (2023). Modeling of Distributed Control System for Network of Mineral Water Wells. (2023).
16. Intergovernmental Panel on Climate Change. (2023). Climate Change 2021 – The Physical Science Basis.
17. J Kittel, E Fleury, S Gonzalez, (2023). Acid gas removal by amine solvents: bridges between CO_2 capture and natural gas treatment. (2023).
18. Jeon, N., Noh, J., Kim, Y. C., Yang, W. S., Ryu, S., & Seok, S. (2014). Solvent engineering for high-performance inorganic-organic hybrid perovskite solar cells. Nature materials.
19. Kuang, T., Zhang, M., Chen, F., Fei, Y., Yang, J., Zhong, M., Wu, B., & Liu, T. (2023). Creating poly (lactic acid)/carbon nanotubes/carbon black nanocomposites with high electrical conductivity and good mechanical properties by constructing a segregated double network with a low content of hybrid nanofiller. Advanced Composites and Hybrid Materials, 6, 1-12.
20. Kumar, C., Kumar, D., Kumar, A., Vikas, K., & Sircar, S. (2023). Coverage of mass drug administration (MDA) and operational issues in elimination of lymphatic filariasis in selected districts of Jharkhand, India. Journal of Family Medicine and Primary Care, 12, 111-116.
21. Liang, Y., Yang, L., Liu, S., Xu, R., Jiang, W., & Wu, P. (2022). Study on the process intensification of superaerophobic materials to improve CO_2 mass transfer efficiency. Chemical Engineering and Processing - Process Intensification.
22. Ma, X., Ran, G., Li, H., Liu, Y., Cui, X., Lu, H., ... Bo, Z. (2023). Modulating the Growth of Nonfullerene Acceptors Toward Efficient and Stable Organic Solar Cells Processed by High-Boiling-Point Solvents. Advanced Energy Materials.

23. Milshtein, J. D., Tenny, K. M., Barton, J., Drake, J., Darling, R., & Brushett, F. (2017). Quantifying Mass Transfer Rates in Redox Flow Batteries. Journal of The Electrochemical Society.
24. Milshtein, J. D., Tenny, K. M., Barton, J., Drake, J., Darling, R., & Brushett, F. (2017). Quantifying Mass Transfer Rates in Redox Flow Batteries. Journal of The Electrochemical Society, 164.
25. Moser, P., Wiechers, G., Schmidt, S., Figueiredo, R. V., Skylogianni, E., & Monteiro, J. G. M. (2023). Conclusions from 3 Years of Continuous Capture Plant Operation Without Exchange of the Amp/Pz-Based Solvent at Niederaussem – Insights into Solvent Degradation Management. SSRN Electronic Journal.
26. Ng, E., Lau, K. K., Chin, S., & Lim, S. (2023). Foam and Antifoam Behavior of PDMS in MDEA-PZ Solution in the Presence of Different Degradation Products for CO_2 Absorption Process. Sustainability.
27. Pan, S., Wang, T., Jin, K., & Cai, X. (2022). Understanding and designing metal matrix nanocomposites with high electrical conductivity: a review. Journal of Materials Science, 57, 6487-6523.
28. Prusti, B., Tripathi, S., Jain, A., & Chakravarty, M. (2023). Concentration-Guided Visual Detection of Multiphase Aliphatic Biogenic Amines through Amine-Phenol Recognition Using a Dual-State Emitter. ACS applied materials & interfaces.
29. Ratman, I., Kusworo, T., & Ismail, A. (2010). Foam Behaviour of An Aqueous Solution of Piperazine- N-Methyldiethanolamine (MDEA) Blend as A Function of The Type of Impurities and Concentrations. International Journal of Science and Engineering, 1, 7-14.
30. Shen, K., Cheng, D., Reyes-Lopez, E., Jang, J., Sautet, P., & Morales-Guio, C. G. (2023). On the origin of carbon sources in the electrochemical upgrade of CO2 from carbon capture solutions.
31. Slameršak, A., Kallis, G., & O'Neill, D. W. (2022). Energy requirements and carbon emissions for a low-carbon energy transition.
32. Sonnichsen, C., Atamanchuk, D., Hendricks, A., Morgan, S., Smith, J., Grundke, I., Luy, E., & Sieben, V. (2023). An Automated Microfluidic Analyzer for In Situ Monitoring of Total Alkalinity. ACS Sensors.
33. Takahashi, T., Koide, H., Sakai, H., Ajito, D., Kurniawan, A., Kunisada, Y., & Nomura, T. (2020). Catalyst-loaded micro-encapsulated phase change material for thermal control of exothermic reaction. Scientific Reports.
34. Tollefson, C., & Gulbrandson, L. (2023). Improving Process Efficiency. Bulan, R., & Oz, F. (2021). Impact of tarragon usage on lipid oxidation and heterocyclic aromatic amine formation in meatball.
35. Triki, M., Herrero, A. M., Jiménez-Colmenero, F., & Ruiz-Capillas, C. (2018). Quality assessment of fresh meat from several species based on free amino acid and biogenic amine contents during chilled storage. Foods.
36. Turan, M. (2023). Backwashing of granular media filters and membranes for water treatment: a review. Journal of Water Supply: Research and Technology-Aqua.

37. Wang, Y.-f., Yang, T., Wang, H.-y., Ding, L., Luo, Y.-f., & Long, H. (2022). Application of steam injection in iron ore sintering: fuel combustion efficiency and CO emissions. Journal of Iron and Steel Research International, 30, 31-39.
38. Yang, D., Zhang, X., Wang, T., Lu, G., & Peng, Y. (2023). Study on pipeline corrosion monitoring based on piezoelectric active time reversal method. Smart Materials and Structures, 32(1), 1-4.
39. Ye, S., Williams, N. X., & Franklin, A. (2022). Aerosol Jet Printing of SU-8 as a Passivation Layer Against Ionic Solutions. Journal of Electronic Materials, 51, 1583-1590.
40. Yuan, W., Huang, X., Fu, J., Ma, Y., Li, G., & Huang, Q. (2022). Water Vapor Blending Ratio Effects on Combustion Thermal Performance and Emission of Hydrogen Homogeneous Charge Compression Ignition. Energies.
41. Zhang, L., Jang, H., Liu, H., Kim, M. G., Yang, D., Liu, S., ... Cho, J. (2021). Sodium-Decorated Amorphous/Crystalline RuO2 with Rich Oxygen Vacancies: A Robust pH-Universal Oxygen Evolution Electrocatalyst. Angewandte Chemie.